SCIENCE CHINA
Physics, Mechanics & Astronomy

• Article •
Special Topic: Fluid Mechanics

February 2013 Vol.56 No.2: 315–321
doi: 10.1007/s11433-012-4980-6

Numerical modeling of oil spill containment by boom using SPH

YANG XiuFeng & LIU MouBin*

Key Laboratory for Mechanics in Fluid Solid Coupling Systems, Institute of Mechanics, Chinese Academy of Sciences, Beijing 100190, China

Received July 2, 2012; accepted September 5, 2012; published online January 21, 2013

The ocean environment is protected from oil pollution usually by using floating booms, which involves water-oil two-phase flow and strong fluid-structure interaction. In this paper, a modified multi-phase smoothed particle hydrodynamics (SPH) method is proposed to model oil spill containment by using a moving boom. Four major influencing factors including oil type, moving velocity and skirt angle of the boom, and water wave are investigated. The SPH simulation results demonstrate different typical boom failure modes found in laboratory experiments. It is shown that the ability of a boom in containing oil is not only affected by its own characteristics, but also closely related to external environmental factors. It is found that boom failure is more likely to happen for heavy oil, high boom velocity, negative skirt angle, and/or in the presence of water waves.

smoothed particle hydrodynamics, oil spill, boom, multi-phase flow

PACS number(s): 47.11.-j, 47.55.-t

Citation: Yang X F, Liu M B. Numerical modeling of oil spill containment by boom using SPH. Sci China-Phys Mech Astron, 2013, 56: 315–321, doi: 10.1007/s11433-012-4980-6

1 Introduction

The world's total oil reserve is around 300 billion tons, among which over 100 billion tons are from offshore oil. During the process of ocean oil extraction and transportation, oil inevitable leaks and spills. According to the statistics of the U.S. National Academy of Sciences, the world annually leaked oil in water is about 170–880 million tons [1]. Oil leakage and spill causes pollution of ocean environment, deaths of marine life and other economic losses on marine and coastal areas. Typical examples including oil spill in the Gulf of Mexico in 2010, and in the Bohai Bay in 2011, both leading to severe environment disaster and tremendous economic losses. Therefore, how to confine the spill of oil after its leakage, and prevent oil from spreading to wider areas is a very important task in ocean engineering.

Booms are the most commonly used equipment to concentrate leaked oil and prevent it from spreading. A boom usually has two main basic parts: an upper freeboard to prevent oil form flowing over the top of the boom, and an immerged skirt to prevent oil from being swept underneath the boom [1]. The performance and ability of a boom to contain oil is affected not only by the characteristics of itself, but also by external environmental factors. The boom's characteristic features include the size and design of the freeboard, the height and angle of the skirt, and the momentum of inertia of the boom. External factors include oil type, water currents, water waves, winds, etc. In some situations, the booms may fail to contain the oil and the oil escapes beneath or over the boom. There are different modes of boom failure, such as entrainment, drainage, critical accumulation, splash-over, submergence, and planing [1,2].

In order to study the mechanism of oil spill containment and boom failure, experiments were carried out in laboratory water flumes. Brown et al. [3] observed oil containment and boom failure in an outdoor flowing water channel and obtained experimental data on boom failure mechanisms. Amini et al. [4] experimentally investigated the instability

*Corresponding author (email: liumoubin@imech.ac.cn)

© Science China Press and Springer-Verlag Berlin Heidelberg 2013

mechanism that can cause the failure of an oil spill barrier. It was reported that the barrier draft and its type are the main factors influencing the velocity in the vicinity of the barrier.

With the rapid development of computer hardware and software as well as numerical methods, numerical simulations of oil spill become gradually popular. However, oil spill in ocean and inland water involves flows with water-oil two-phase flows with free surfaces, and containing oil spill using boom involves strong fluid-structure interaction. Both two-phase and free surface flows, and fluid-solid interaction are important but formidable tasks for numerical simulations as conventional grid-based numerical methods are difficult in simultaneously treating moving and deformable solid objects when tracking free surfaces and fluid interfaces. Currently, existing numerical simulations of oil spill are mainly conducted using commercial CFD software, such as FLUENT and CFX, in which free surfaces are usually treated as slip walls and the boom does not move [2,5–7]. The obtained numerical results are therefore different from practical problems.

In this paper, smoothed particle hydrodynamics (SPH) method is applied to model oil spill and boom movement. SPH is a meshfree Lagrangian particle method [8–11]. As a meshfree particle method, SPH is suitable for modeling problems with free surfaces, moving interfaces, deformable boundaries and large deformations [8–10,12]. SPH was originally invented to solve astrophysical problems in open space [13,14] and it was later extended to simulate many other compressible flows such as shock problems [8–10,12, 15]. By treating the flow as slightly compressible with an appropriate equation of state, the SPH method can be used to simulate incompressible flows successfully [16,17]. It is also possible to rigorously treat incompressible flows in SPH through solving the pressure Poisson equation [18,19] in a way similar to the moving particle semi-implicit (MPS) method [20,21]. SPH was also extended to simulate multi-phase flows [22–24]. Violeau et al. [25] once studied the mechanism of oil leakage by entrainment using conventional SPH and obtained some preliminary results.

The paper is organized as follows. In the next section, a modified SPH method is presented for simulating water-oil two-phase flow. In sect. 3, the modified SPH method is applied to simulate oil containment and boom failure with main influencing factors including oil type, boom velocity, skirt angle, and waves. The paper ends in sect. 4 with some discussions and conclusions.

2 Multi-phase SPH method

2.1 SPH approximation

In SPH, a continuous field is represented by a set of particles (or points). The particles carry physical properties such as mass m, density ρ, volume $V=m/\rho$, and velocity $\boldsymbol{u}$. The value of a field function $f(\boldsymbol{r})$ at a space point $\boldsymbol{r}_a$ can be obtained from its neighboring particles as follows:

$$f_a = \sum_b f_b V_b W(\boldsymbol{r}_a - \boldsymbol{r}_b, h), \tag{1}$$

where $f_a \equiv f(\boldsymbol{r}_a)$, the function W is called kernel, weight or smoothing function, and subscripts a and b denote particles at points $\boldsymbol{r}_a$ and $\boldsymbol{r}_b$, respectively. Parameter h is the smoothing length that is closely related to the influencing area of the kernel function. The summation is over all the particles. But in practice, it is conducted only over the nearest neighbors around particle a because of the compact supportness of the kernel function, which causes the kernel function to fall off rapidly with the increase of particle spacing $|\boldsymbol{r}_a-\boldsymbol{r}_b|$. The kernel W is also assumed to be an even function with respect to $\boldsymbol{r}_a-\boldsymbol{r}_b$ and normalized to 1. A commonly used kernel is the cubic spline

$$W(s,h) = \alpha \begin{cases} (2-s)^3 - 4(1-s)^3, & 0 \leqslant s < 1, \\ (2-s)^3, & 1 \leqslant s < 2, \\ 0, & s \geqslant 2, \end{cases} \tag{2}$$

where $s \equiv |\boldsymbol{r}_a-\boldsymbol{r}_b|/h$ and α is the normalization factor with the value of $5/(14\pi h^2)$ in two-dimensional space.

The gradient of function f can be obtained by differentiating equation (1) exactly,

$$\nabla f_a = \sum_b V_b f_b \nabla_a W_{ab}, \tag{3}$$

where $\nabla_a W_{ab} = W'_{ab}\, \boldsymbol{r}_{ab}/r_{ab}$ is the gradient of the kernel taken with respect to the position of particle a. Here $\boldsymbol{r}_{ab} \equiv \boldsymbol{r}_a-\boldsymbol{r}_b$ is the displacement vector from particle a to particle b, and r_{ab} ($\equiv|\boldsymbol{r}_{ab}|$) is the distance between particles a and b. More details of kernel approximation of derivatives can be found in a number of reports [9,11,12].

It is well known that SPH simulation can meet numerical instability under a certain stress state. This stress instability is frequently observed in solid dynamics problems, especially hydrodynamics with material strength and is usually referred to as tensile instability. There is obvious evidence that stress instability also happens for fluid flow problems. It is reported that the stress instability depends on the sign of the multiplication of the stress and the second derivative of the kernel function [26]. Instability occurs when the product is positive. In standard SPH, bell-shaped kernels are frequently used. The second derivative of a bell-shaped kernel, such as the cubic spline (see Figure 1), changes sign from negative to positive so that the product of the stress times the second derivative of the kernel function will change sign whether the stress is positive or negative. That means if bell-shaped kernel functions are used, stress instability is almost inevitable.

In order to prevent instability, a new cubic kernel was

used,

$$W(s,h)=\alpha\begin{cases}s^3-6s+6, & 0\leqslant s<1,\\ (2-s)^3, & 1\leqslant s<2,\\ 0, & 2\leqslant s,\end{cases} \tag{4}$$

where α=1/(3πh^2) in two-dimensional space. Because the second derivative of the new cubic kernel (see Figure 2) is non-negative and the stress in fluids is non-positive (the sign of the stress is opposite to pressure, which is always positive in fluids), the product is also non-positive. Therefore by using this new kernel function, stress instability can be effectively removed for fluid flow problems.

2.2 Governing equations

The Reynolds-averaged Navier-Stokes (RANS) equations are written in Lagrangian form as follows:

$$\frac{\mathrm{d}\rho}{\mathrm{d}t}=-\rho\nabla\cdot\boldsymbol{u}, \tag{5}$$

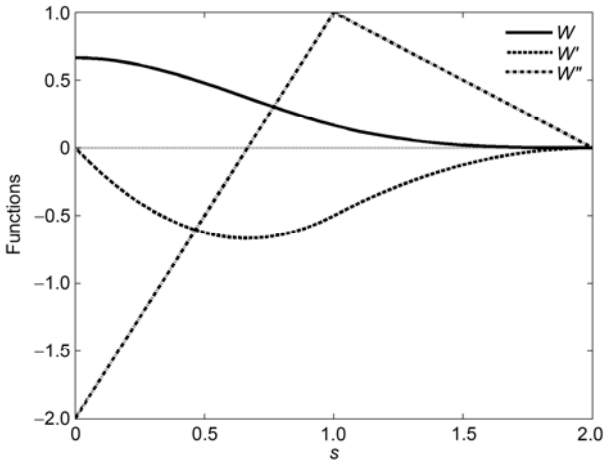

Figure 1 The shape of the cubic spline kernel and its first and second derivatives.

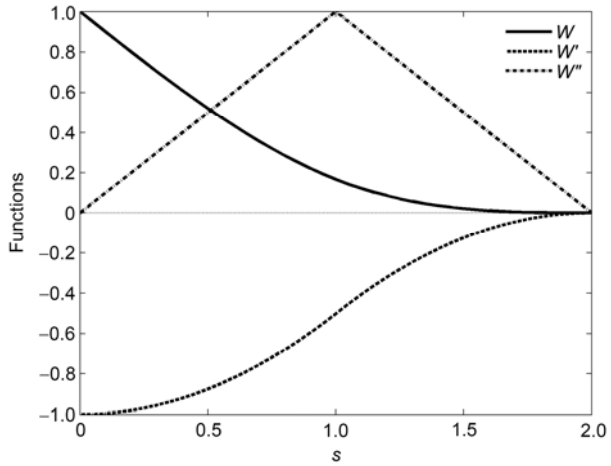

Figure 2 The shape of the new cubic kernel and its first and second derivatives.

$$\frac{\mathrm{d}\boldsymbol{u}}{\mathrm{d}t}=\boldsymbol{g}-\frac{1}{\rho}\nabla p+\nu\nabla^2\boldsymbol{u}-\frac{1}{\rho}\nabla\cdot(\rho\boldsymbol{R}), \tag{6}$$

where ρ is fluid density, $\boldsymbol{u}$ is the Reynolds-averaged velocity vector, p is the Reynolds-averaged pressure, ν is the kinetic viscosity, $\boldsymbol{g}$ denotes the gravitational acceleration, $\boldsymbol{R}$ denotes the Reynolds stress tensor with elements given by $R_{ij}=\overline{u_i'u_j'}$, where u' denotes velocity turbulent fluctuation and the overstrike bar means Reynolds-averaged. It should be noted that subscripts i and j denote spatial coordinates while subscripts a and b denote particles in this work.

The Reynolds stress tensor can be modeled through the traditional eddy viscosity assumption as:

$$\boldsymbol{R}=\frac{2}{3}k\boldsymbol{I}-2\nu_t\boldsymbol{S}, \tag{7}$$

where $k\equiv\overline{u_i'u_i'}/2$ is the turbulent kinetic energy, ν_t is an eddy viscosity, and $\boldsymbol{S}$ is the mean rate of strain tensor with elements given by

$$S_{ij}=\frac{1}{2}\left(\frac{\partial u_j}{\partial x_i}+\frac{\partial u_i}{\partial x_j}\right). \tag{8}$$

The Smagorinsky eddy viscosity model is used to obtain eddy viscosity

$$\nu_t=l^2\sqrt{2S_{ij}S_{ij}}, \tag{9}$$

where l is a mixing length. In SPH, the mixing length can be assumed to be the sub-particle characteristic length scale given by l=$C_s l_p$, where l_p is the particle spacing and C_s is Smagorinsky constant with a range of 0.1–0.24 [27,28].

Using the kernel approximation as shown in eqs. (1) and (3), the RANS equations in SPH form can be obtained. The continuity equation (5) can be written in two SPH forms:

$$\frac{\mathrm{d}\rho_a}{\mathrm{d}t}=\rho_a\sum_b V_b\boldsymbol{u}_{ab}\cdot\nabla_a W_{ab}, \tag{10}$$

and

$$\frac{\mathrm{d}\rho_a}{\mathrm{d}t}=\sum_b m_b\boldsymbol{u}_{ab}\cdot\nabla_a W_{ab}, \tag{11}$$

where $\boldsymbol{u}_{ab}\equiv\boldsymbol{u}_a-\boldsymbol{u}_b$. Both equations can be used for fluid simulations. The main difference between them is that eq. (11) involves density explicitly while eq. (10) does not. Eq. (11) performs better for incompressible flows, but eq. (10) performs better for interface flows [9]. Considering the different advantages of both equations, a mixed form of continuity equation is used in this paper for multi-phase, incompressible free surface flows:

$$\frac{\mathrm{d}\rho_a}{\mathrm{d}t}=\sum_{b\subset A} m_b\boldsymbol{u}_{ab}\cdot\nabla_a W_{ab}+\rho_a\sum_{b\not\subset A} V_b\boldsymbol{u}_{ab}\cdot\nabla_a W_{ab}, \tag{12}$$

where $b \subset A$ means that both particles b and a are from the same fluid phase A, and $b \not\subset A$ means that particle b is from a fluid phase different from fluid phase A, which contains the concerned particle a.

The SPH formulations for the last three parts on the right hand side of the momentum equation (6) can be written separately as follows:

$$\left(\frac{1}{\rho}\nabla p\right)_a = \sum_b (1+C_{ab}) m_b \left(\frac{p_a}{\rho_a^2}+\frac{p_b}{\rho_b^2}\right)\nabla_a W_{ab}, \tag{13}$$

$$\left(\nu\ \nabla^2 \boldsymbol{u}\right)_a = \sum_b \frac{m_b(\mu_a+\mu_b)\boldsymbol{r}_{ab}\cdot\nabla_a W_{ab}}{\rho_a\rho_b(r_{ab}^2+\eta)}\boldsymbol{u}_{ab}, \tag{14}$$

$$\frac{1}{\rho}\nabla\cdot(\rho\boldsymbol{R})_a = \sum_b m_b\left(\frac{\boldsymbol{R}_a}{\rho_a}+\frac{\boldsymbol{R}_b}{\rho_b}\right)\nabla_a W_{ab}, \tag{15}$$

where $\mu=\rho\nu$, $\eta=0.01h^2$, and parameter C_{ab} is a constant used to prevent particle penetration from one phase to another. It is defined as:

$$C_{ab} = \begin{cases} 0, & b \subset A, \\ C_{\mathrm{p}}, & b \not\subset A, \end{cases} \tag{16}$$

where parameter $C_{\mathrm{p}}>0$. In this paper, a value of 0.2 is found to be suitable.

In SPH, an artificial compressibility technique is usually used to model the incompressible flow as a slightly compressible flow. The artificial compressibility considers that every theoretically incompressible fluid is actually slightly compressible. Therefore, it is feasible to model the incompressible flow by using a quasi-incompressible equation of state [17]

$$p(\rho) = c^2(\rho-\rho_0), \tag{17}$$

where ρ_0 is a reference density with a different value for a different fluid, and c is a numerical speed of sound. In order to reduce the density fluctuation down to one percent, the numerical speed of sound c is set to be ten times or larger than the maximum fluid velocity. In the case of hydrostatic fluid, the maximum fluid velocity can be estimated by $u_{\max}=\sqrt{2gH}$, where g is the gravitational acceleration and H is the maximum water depth.

In SPH simulations, there may be large fluctuation in the pressure field of particles because the density error accumulates when time marches. In order to reduce the fluctuation, the density field can be reinitialized every tens of time steps by Shephard filtering

$$\tilde{\rho}_a = \frac{\sum_b m_b W_{ab}}{\sum_b W_{ab} V_b}. \tag{18}$$

2.3 Boundary conditions

There are two types of boundaries which should be carefully considered when modeling oil spill containment, free surface and solid boundary.

Since there are no particles in the outer region of a free surface, if the pressure of free surface particles is bigger than zero, the distance between particles will become larger and this causes numerical fluctuations. In order to prevent this kind of numerical fluctuations, density will be set to reference density ρ_0 if a particle is on or near the free surface, and hence its pressure will be zero according to the artificial equation of state (17). In this work, a particle which satisfies

$$\sum_b W_{ab} V_b < \beta, \tag{19}$$

is considered as a surface particle, where parameter $\beta<1$. In the following numerical examples we take $\beta=0.9$. The free surface treatment used here is similar to the approach used in MPS method [20,21].

Solid boundary can be treated easily by replacing the boundary with particles which interact with fluid particles. There are kinds of solid boundary treatment methods. Some authors prefer to impose artificial repulsive force between fluid particles and boundary particle directly which is referred to as repulsive boundary while others prefer to calculate the interaction by considering the boundary particles as they are fluid particles which is referred to as dynamic boundary. The latter gives fewer disturbances to the fluid flow, but it is not easy to be applied to multi-phase fluid. In this paper, the following force derived from the momentum equation can be used to estimate the interaction between fluid and solid particles

$$\boldsymbol{f}_{ab} = \frac{2V_b}{\rho_a}\left(p_a\nabla_a W_{ab} + \frac{\mu_a \boldsymbol{r}_{ab}\cdot\nabla_a W_{ab}}{r_{ab}^2}\boldsymbol{u}_{ab}\right). \tag{20}$$

According to Newton's third law, the force acting on a boundary particle from a fluid particle is

$$\boldsymbol{F}_{ba} = -\boldsymbol{F}_{ab} = -m_a \boldsymbol{f}_{ab}. \tag{21}$$

And the total force acting on a boom is

$$\boldsymbol{F} = \sum_{a,b} \boldsymbol{F}_{ba}, \tag{22}$$

where the summation is taken over all boom particles b and fluid particle a which interacted with boom particles. The motion of a boom follows from Newton's second law

$$\frac{\mathrm{d}U}{\mathrm{d}t} = \frac{\boldsymbol{F}}{M}, \tag{23}$$

where U and M are the boom velocity and mass, respectively.

3 Numerical examples

3.1 Numerical water flume

Numerical simulations are carried out in a numerical water flume. As shown in Figure 3, the length of the numerical

flume is 18 m, and the water depth is 2.5 m. There is a wave maker (① in Figure 3) to make wave for investigating wave effects on oil spill containment, and wave-making is implemented by rotating the wave maker at a specific angle and frequency. ② in Figure 3 shows an oil inlet while a certain amount of oil leaks at a specific speed for a period of time before the boom arrives at the vicinity of the oil inlet. The boom (③ in Figure 3) moves leftwards at a constant horizontal velocity U_b controlled by a towing ship, and it can move freely in the vertical direction. The height of skirt is 0.75 m and the boom skirt angle refers to the angle between the boom skirt and the vertical direction.

In order to absorb the reflected wave energy from the outlet end of the flume, a layer of porous media was set in front of the right end of the flume (④ in Figure 3). The flow in porous media can be described by the following equation [29]:

$$\frac{\mathrm{d}\boldsymbol{u}}{\mathrm{d}t} = \boldsymbol{g} - \frac{1}{\rho}\nabla p + \nu\nabla^2\boldsymbol{u} - \frac{\nu n_w}{K_p}\boldsymbol{u} - \frac{C_f n_w^2}{\sqrt{K_p}}u\boldsymbol{u}, \tag{24}$$

where parameters K_p and C_f are defined as:

$$K_p = 1.643\times10^{-7}\frac{n_w^3}{(1-n_w)^2}\left(\frac{d}{d_0}\right)^{1.57}, \tag{25}$$

$$C_f = 100\left(d\sqrt{\frac{n_w}{K_p}}\right)^{-1.5}, \tag{26}$$

where d_0=0.01 m. In all the following simulations in this paper we take d=0.05 m, n_w=0.5, and then from eqs. (25) and (26) we have K_p=1.0×10^{-6}, C_f= 0.5. By using the layer of porous media, reflected wave energy can be effectively absorbed.

3.2 Results of the numerical simulation

In this section, oil spill containment was numerically simulated under various situations using an in-house SPH code with modified algorithms in improving computational accuracy and enhancing boundary treatment. Oil spill containment is a very complex process involving water-oil two-phase flows and fluid-structure interaction with free surfaces, deformable interfaces and moving structures. It's therefore difficult for numerical simulations and there are very limited reports in simulating oil spill and boom movement. It is even more difficult to give quantitatively agreeable results with experimental observations. As the effectiveness of the in-house SPH code with modified algorithms has been demonstrated in a wide range of applications with free surfaces, moving interfaces and fluid-structure interaction [30,31], it is used to investigate the oil spill containment with different influencing factors. In this work, about 20000 fluid particles are used, and four major factors including oil type, boom velocity, skirt angle, and water waves are considered. Two types of oil, the same as those in ref. [25], are used, and the related properties (density and viscosity) are listed in Table 1.

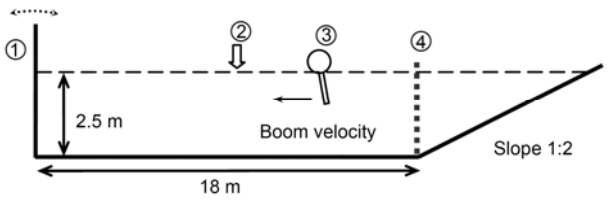

Figure 3 Sketch of the numerical flume. ① wave maker, ② oil inlet, ③ boom, ④ porous media for absorbing wave energy.

3.2.1 *Effect of oil type*

Different types of oil can lead to different flow and spill performances that require different treatments when oil spill is contained with boom. In order to investigate the influence of oil type in oil spill containment, both light oil and heavy oil are studied without considering water wave. In the simulation, the skirt angle is taken as 10° and boom velocity is 0.7 m/s leftwards.

Figure 4 shows the flow pattern evolution of oil layer and the velocity field of water flow at different typical instants. When a certain amount of oil leaks from the oil inlet, it gradually accumulates near the leaking area, and spills outwards. When the boom moves to the left, the water underneath the boom moves to the right. Therefore for both light and heavy oil, a vortex is formed around the boom with the vertex center located right behind the boom.

As the density of light oil is smaller than that of water, an oil layer over the water surface forms. When the boom moves leftwards, at the very beginning, a small portion of oil can escape underneath the boom. With the advancement of the boom, the oil layer becomes longer and thinner, and boom failure (oil escapement) does not happen again (see Figure 4, left column). In contrast, as the density of heavy oil is close to that of water, it is more likely to form a shorter but thicker oil layer. Hence it is more likely for a boom with the same skirt angle and moving velocity to fail in containing the spilled oil (see Figure 4, right column). It also can be observed that heavy oil frequently escapes from the bottom of the boom. This boom failure is a mixed form of entrainment and drainage.

3.2.2 *Effect of the boom velocity*

In this subsection, the performance of heavy oil spill containment with two different boom velocities, 0.3 m/s and 0.7 m/s, are numerically simulated to investigate the effects of boom velocity while the skirt angle is taken as 0°, and the

Table 1 Parameters of oil and water

Type of oil	ρ (kg·m^{-3})	ν (m^2·s^{-1})
Light oil	850	3.32×10^{-6}
Heavy oil	995	3.00×10^{-2}
Water	1000	1.00×10^{-6}

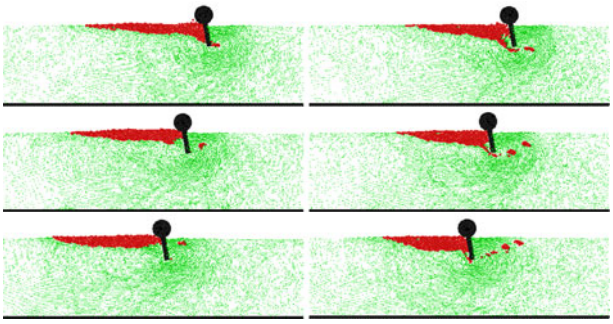

Figure 4 (Color online) Oil spill containment for light oil (left) and heavy oil (right), skirt angle 10°, boom velocity 0.7 m/s.

water wave is not considered. Figure 5 shows the flow pattern evolution of oil layer and the velocity field of water for these two different boom velocities. It is clear that when the boom moves at 0.3 m/s, the spilled oil does not escape and boom failure does not happen (see Figure 5, left column). Instead, when a boom moves at a higher velocity, it is more likely to form a thicker oil layer in front of the boom and it is therefore more likely for the accumulated oil to escape from the bottom of the boom (see Figure 5, right column). This is a mixed form of boom failure with drainage and accumulation. It is also observed that a boom with higher velocity can lead to a stronger vortex around the boom.

3.2.3 *Effect of the skirt angle*

For different flow simulations, the skirt angle can be changed to meet the needs of oil spill containment. In this subsection, the effects of skirt angle in containing oil spill are investigated for light oil, with a boom velocity of 0.7 m/s. Water wave effects are not considered. Figure 6 shows the flow pattern evolution of oil layer and the velocity field of water for two skirt angles, –30° and 30°. It is obvious that different deployment of the boom can result in quite different performances in oil spill containment. Different skirt angles lead to different flow fields, especially around the boom. For a negative skirt angle, the flow velocity (direction and magnitude) of the water and oil right in front of the boom is close to the velocity of the boom, so it is easier for the oil layer to become longer and thinner. Hence the spilled oil does not escape and boom failure does not happen (see Figure 6, left column). In contrast, for a positive skirt angle, the flow direction of the water and oil right in front of the boom is different from the direction of the boom movement; it is therefore more likely for oil to escape from the bottom of the boom (see Figure 6, right column). This boom failure is planing.

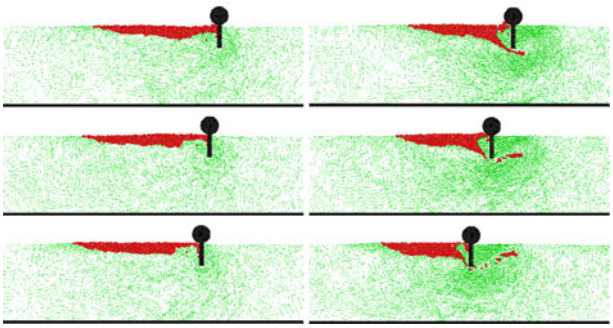

Figure 5 (Color online) Oil spill containment with two boom velocities, 0.3 m/s (left) and 0.7 m/s (right), heavy oil, skirt angle 0°.

3.2.4 *Effect of waves*

For oil spill in ocean environment, wave effects can be very important. In order to make waves, the rotational angle of the wave maker (① in Figure 3) in degrees is $\theta=6\sin(\pi t)$, and the period is 2 s. Figure 7 shows the flow pattern evolution of oil layer and the velocity field of water for heavy oil spill containment with and without considering wave effects, while the skirt angle is 0° and the boom velocity is 0.5 m/s. There is no boom failure when water wave is not considered (see Figure 7, left column). It is revealed that water wave is significant in affecting the flow pattern and velocity field (see Figure 7, right column). With the advancement of the water wave, the spilled oil layer and boom can move upwards and downwards. If some oil is in a position above the boom, it can escape from the top of the boom (splashover). In contrast, if some oil is in a position below the boom, it can escape from the bottom of the boom (accumulation). More importantly, boom failure periodically happens with the periodical interaction of the water wave and the boom. Therefore, in order to effectively contain oil spill in an environment with water waves, a more suitable design of the

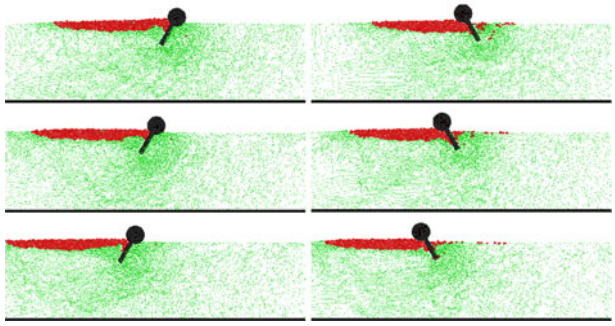

Figure 6 (Color online) Oil spill containment with two skirt angles, –30° (left) and 30° (right), light oil, boom velocity 0.7 m/s.

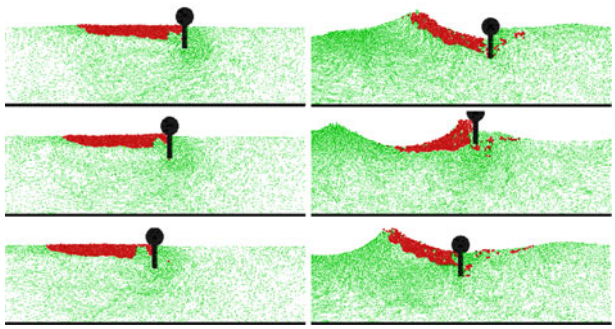

Figure 7 (Color online) Oil spill containment without (left) and with (right) wave effects, heavy oil, skirt angle 0°, boom velocity 0.5 m/s.

boom is necessary.

4 Conclusions

This paper presents a numerical simulation of oil spill containment by boom using SPH method. In order to simulate oil spill and boom movement, a modified SPH method is proposed, which can effectively treat water-oil two-phase flows and fluid-structure interaction with free surfaces, deformable interfaces and moving structures. Major modifications include a new kernel function for removing numerical instability, mixed form of SPH equations for two-phase flow, and enhanced boundary treatment method for better accuracy and flexibility.

Four major factors influencing oil spill containment including oil type, moving velocity and skirt angle of the boom and water wave are investigated. It is found that when other influencing factors are determined, boom failure is more likely to happen for situations with heavy oil, fast boom velocity, negative skirt angle and water waves. It is noted that the present observations are basically qualitative, and future work will include more quantitative comparisons with laboratory experiments and/or field tests. More influencing factors and more types of boom for oil spill containment will also be investigated.

This work was supported by the National Natural Science Foundation of China (Grant No. 11172306) and the Program of "One Hundred Talented People" of the Chinese Academy of Sciences.

1 Fingas M. Oil Spill Science and Technology: Prevention, Response, and Cleanup. Burlington: Gulf Professional Publishing, 2011
2 Goodman R H, Brown H M, An C F, et al. Dynamic modelling of oil boom failure using computational fluid dynamics. Spill Sci Technol Bull, 1996, 3: 213–216
3 Brown H M, Goodman R H, An C F, et al. Boom failure mechanisms: Comparison of channel experiments with computer modelling results. Spill Sci Technol Bull, 1996, 3: 217–220
4 Amini A, De Cesare G, Schleiss A J. Velocity profiles and interface instability in a two-phase fluid: Investigations using ultrasonic velocity profiler. Exp Fluids, 2009, 46: 683–692
5 Amini A, Schleiss A J. Numerical modeling of oil-water multiphase flow contained by an oil spill barrier. Eng Appl Comput Fluid Mech, 2009, 3: 207–219
6 Ning C, Zhang Z. Numerical simualtion of oil-boom failure with CFX4.3. J Beijing Univ Chem Technol, 2002, 29: 25–29
7 Fang X, Wu W, Wu W. Numerical simulation technology of oil containment by boom. In: 2011 2nd International Conference on Environmental Science and Technology, Conference Place. Singapore: IACSIT Press, 2011. 6
8 Liu M B, Liu G R. Smoothed Particle Hydrodynamics (SPH): An overview and recent developments. Arch Comput Methods Eng, 2010, 17: 25–76
9 Monaghan J J. Smoothed particle hydrodynamics. Rep Prog Phys, 2005, 68: 1703–1759
10 Cleary P W, Prakash M, Ha J, et al. Smooth particle hydrodynamics: Status and future potential. Prog Comput Fluid Dyn, 2007, 7: 70–90
11 Monaghan J J. Smoothed particle hydrodynamics. Annu Rev Astron Astrophys, 1992, 30: 543–574
12 Liu G R, Liu M B. Smoothed Particle Hydrodynamics: A Meshfree Particle Method. Singapore: World Scientific, 2003
13 Lucy L B. A numerical approach to the testing of the fission hypothesis. Astron J, 1977, 82: 1013–1024
14 Gingold R A, Monaghan J J. Smoothed particle hydrodynamics: Theory and application to non-spherical stars. Mon Not R Astron Soc, 1977, 181: 375–389
15 Monaghan J J, Gingold R A. Shock simulation by the particle method SPH. J Comput Phys, 1983, 52: 374–389
16 Monaghan J J. Simulating free surface flows with SPH. J Comput Phys, 1994, 110: 399–406
17 Morris J P, Fox P J, Zhu Y. Modeling low Reynolds number incompressible flows using SPH. J Comput Phys, 1997, 136: 214–226
18 Edmond Y M L, Shao S. Simulation of near-shore solitary wave mechanics by an incompressible SPH method. Appl Ocean Res, 2002, 24: 275–286
19 Shao S, Lo E Y M. Incompressible SPH method for simulating Newtonian and non-Newtonian flows with a free surface. Adv Water Res, 2003, 26: 787–800
20 Koshizuka S, Oka Y. Moving-particle semi-implicit method for fragmentation of incompressible fluid. Nucl Sci Eng, 1996, 123: 421–434
21 Koshizuka S, Nobe A, Oka Y. Numerical analysis of breaking waves using the moving particle semi-implicit method. Intl J Numer Methods Fluids, 1998, 26: 751–769
22 Colagrossi A, Landrini M. Numerical simulation of interfacial flows by smoothed particle hydrodynamics. J Comput Phys, 2003, 191: 448–475
23 Hu X Y, Adams N A. An incompressible multi-phase SPH method. J Comput Phys, 2007, 227: 264–278
24 Grenier N, Antuono M, Colagrossi A, et al. An Hamiltonian interface SPH formulation for multi-fluid and free surface flows. J Comput Phys, 2009, 228: 8380–8393
25 Violeau D, Buvat C, Abed-Meraim K, et al. Numerical modelling of boom and oil spill with SPH. Coast Eng, 2007, 54: 895–913
26 Swegle J W, Hicks D L, Attaway S W. Smoothed particle hydrodynamics stability analysis. J Comput Phys, 1995, 116: 123–134
27 Lo E Y M, Shao S. Simulation of near-shore solitary wave mechanics by an incompressible SPH method. Appl Ocean Res, 2002, 24: 275–286
28 Rogallo R S, Moin P. Numerical simulation of turbulent flows. Annu Rev Fluid Mech, 1984, 16: 99–137
29 Huang C J, Chang H H, Hwung H H. Structural permeability effects on the interaction of a solitary wave and a submerged breakwater. Coast Eng, 2003, 49: 1–24
30 Yang X F, Peng S L, Liu M B, et al. Numerical simulation of ballast water by SPH method. Intl J Comput Methods, 2012, 9: 1240002
31 Shao J R, Li H Q, Liu G R, et al. An improved SPH method for modeling liquid sloshing dynamics. Comput Struct, 2012, 100-101: 18–26